Deciphering and Handling Uncertainty in Shale Gas Supply Chain Design and Optimization: Novel Modeling Framework and Computationally Efficient Solution Algorithm

Jiyao Gao and Fengqi You
Dept. of Chemical and Biological Engineering, Northwestern University, Evanston, IL 60208

DOI 10.1002/aic.15032
Published online September 17, 2015 in Wiley Online Library (wileyonlinelibrary.com)

The optimal design and operations of shale gas supply chains under uncertainty of estimated ultimate recovery (EUR) is addressed. A two-stage stochastic mixed-integer linear fractional programming (SMILFP) model is developed to optimize the levelized cost of energy generated from shale gas. In this model, both design and planning decisions are considered with respect to shale well drilling, shale gas production, processing, multiple end-uses, and transportation. To reduce the model size and number of scenarios, we apply a sample average approximation method to generate scenarios based on the real-world EUR data. In addition, a novel solution algorithm integrating the parametric approach and the L-shaped method is proposed for solving the resulting SMILFP problem within a reasonable computational time. The proposed model and algorithm are illustrated through a case study based on the Marcellus shale play, and a deterministic model is considered for comparison. © 2015 American Institute of Chemical Engineers *AIChE J*, 61: 3739–3755, 2015
Keywords: shale gas, supply chain, estimated ultimate recovery, uncertainty, stochastic program, stochastic mixed-integer linear fractional programming

Introduction

In recent years, the widespread application of horizontal drilling and hydraulic fracturing has led to a "shale revolution," which further results in the U.S. transitioning from an importer to a net exporter of natural gas.[1] As reported by the Annual Energy Outlook 2015 released by the U.S. Energy Information Administration (EIA),[2] natural gas production is expected to grow by an average rate of 1.6% per year from 2012 to 2040, more than double the 0.8% expected annual growth rate of total consumption in the U.S. over the same period. The 56% increase in total natural gas production is mainly due to increased shale gas production, which will grow by more than 10 Trillion Standard Cubic Feet (Tscf). The percentage of the U.S. total natural gas production from shale gas is expected to increase from 40% in 2012 to 53% in 2040.

Despite the optimistic forecast of shale gas production given by the EIA, a recent report by Post Carbon Institute unveils the fact that the actual future of shale gas may not be as bright as the EIA suggests.[3] From a well-by-well-based calculation of shale gas production throughout the U.S., they conclude that the actual profitability of a shale well can be significantly affected by the uncertainty in the estimated ultimate recovery (EUR) and astounding decline rates of production ranging from 60 to 90% in the first 3 years. Considering the significant influence of the shale gas industry on the overall U.S. energy sector, it is essential to design and operate emerging shale gas supply chains with explicit consideration of EUR uncertainty and actual shale gas production profiles.

Supply chain design and optimization under uncertainty has long been known as a challenging problem that is vital to the success of industrial concerns.[4,5] Currently, there are publications regarding design and operations of shale gas supply chains,[6–9] and some works present a general analysis of the uncertainty in shale gas supply chains,[10–13] while only a few of them provide a quantitative solution using mathematical programming tools. Yang and Grossmann[14] presented a mixed-integer linear programming (MILP) model optimizing water use life cycle for shale wells. Cafaro and Grossmann[15] proposed a mixed-integer nonlinear programming (MINLP) model to determine the optimal design of a shale gas supply chain. However, operational decisions are not addressed, and the actual lifetime of shale wells are not properly addressed. Gao and You[16] proposed a mixed-integer linear fractional programming (MILFP) model to address the optimal design and operations of a shale water supply chain. Yang and Grossmann[17] presented a new MILP model for optimizing capital investment decisions for water use for shale gas production through a State-Task Network. Recently, Gao and You[18] conducted a life cycle optimization of the shale gas supply chain addressing both design and operational decisions to reveal the trade-off between economic performance and green house gas (GHG) emissions. By reviewing the existing works, we have identified the absence of a comprehensive shale gas supply chain model that considers design and planning decisions under uncertainty. Meanwhile, recently published papers on the life cycle assessment of shale gas highlights the large influence of EUR uncertainty, identified as the most critical source

Correspondence concerning this article should be addressed to F. You at you@northwestern.edu.

of uncertainty that can significantly influence both the economic and environmental performances of shale gas supply chains.[8,19–21] Therefore, we consider it necessary and important to develop a shale gas supply chain model that not only considers both design and planning decisions but also properly addresses EUR uncertainty.

To achieve this goal, the following challenges need to be addressed. First, it is necessary to select the correct data and approach to decipher EUR uncertainty. The second challenge is to develop a novel and comprehensive model based on the EUR distribution that can optimize the economic performance regarding both design and planning decisions under uncertainty. Finally, we need to be able to solve the resulting large-scale optimization problem in a reasonable amount of time. In this work, we derive the EUR distribution based on real data reported in existing literature.[1,22] There are two methods commonly applied to handle uncertainty in optimization problems.[23] The first one involves Robust Optimization (RO) methods.[24,25] Although RO is known for its superior computational tractability, it is designed to address optimization problems with uncertain data that are only known to belong to some uncertainty set. Moreover, because RO considers the worst case, it may suffer from its conservativeness and fail to give an economically attractive optimal solution. By reviewing the reported EUR data as shown in Figure 4, we identify a wide distribution of EUR with distinct "long tails," which is not suitable for applying RO approach. Therefore, we adopt the scenario-based stochastic programming approach to explicitly account for the EUR uncertainty. Stochastic programming has been widely used to quantitatively account for uncertainty in design, planning, and scheduling problems.[26–28] A two-stage SMILFP model is hereby proposed to minimize the levelized cost of energy (LCOE) in a shale gas supply chain. The objective is to find a solution with the best expected performance under all scenarios. Due to the dependence of stochastic programming on the scenarios, the resulting problem size may increase exponentially as the number of scenarios increases. To tackle this challenge, we adopt a sample average approximation (SAA) approach to generate scenarios based on the real-world EUR distribution data.[29] This is combined with statistical methods to determine the required number of scenarios to achieve the desired accuracy.[30,31] The required number of scenarios is significantly reduced with guaranteed solution quality due to the SAA method. To further boost the solution process of the resulting two-stage SMILFP problem, a novel algorithm integrating the parametric approach and the L-shaped method is developed to solve large-scale problems efficiently. Finally, a case study based on the Marcellus shale play is presented to illustrate the application of the proposed modeling framework and solution approaches.

The major novelties of this work are summarized as follows:

- This article is the first work that explicitly addresses EUR uncertainty in the design and operations of shale gas supply chains;
- A novel modeling framework addressing the economic efficiency of shale gas supply chain with multiple end customers taken into account is developed;
- Novel solution algorithms targeting on the solution of two-stage SMILFP problem efficiently are presented;
- A practical case study of a shale gas supply chain based on real-world data from the Marcellus shale play is provided.

The rest of this article is organized as follows. In the following section, we provide the background on a general shale gas supply chain. After that, the formal problem statement is given, followed by the detailed model formulation. Then the SAA method and the proposed novel algorithm are introduced. To illustrate the application of the proposed model and solution method, one case study based on the Marcellus shale play is presented before the conclusion of the work.

Background and Literature Review

A typical shale gas supply chain network is depicted in Figure 1. As can be seen, a shale gas supply chain can be divided into upstream, midstream, and downstream sections.[7]

The upstream section involves all the phases that are directly or indirectly related to shale gas production activities at shale sites. There are preparation phases including potential well exploration, leasing, acquisition, and permitting. Well exploration is the very first phase in the shale gas supply chain, where potential drilling sites are identified based on geologic evaluations. Once this phase is completed, the shale well operator must sign corresponding lease contracts and obtain necessary permits following existing policy and regulations. After the preparation phases, shale site infrastructure can be installed and drilling activities can start. Typical shale site infrastructure includes mud ponds, drilling rigs, brine storage tanks, onsite processing equipment, mobile wastewater treatment facilities, transportation trucks, and so forth. The drilling process normally consists of multiple stages, and each stage involves corresponding steel casing inserting and cement injection. After the drilling process, hydraulic fracturing, also known as "fracking," is implemented. Millions of gallons of fracturing fluid as a mixture of water, sand, and chemical additives is injected into the wellbore under high pressure, such that fractures are created and are kept open by proppant trapped in the fractures after fracturing water pressure is released, and shale gas flows back to the surface as a raw product. Together with the shale gas, a certain percentage of water flows back as highly contaminated wastewater that can either be treated, disposed of, or reused. Corresponding water management options include Class-II disposal wells, centralized wastewater treatment facilities, and onsite treatment.[32] The raw shale gas, depending on specific shale play location, generally has a different composition.

After a simple preprocessing step to satisfy the pipeline requirement, the shale gas will be compressed and transported to processing plants for further separation, identified as the midstream section of the shale gas supply chain. A typical design for a conventional shale gas processing plant includes the following processes: acid removal, sulfur recovery and tail gas cleanup, dehydration, natural gas liquids (NGLs) recovery, fractionation, and nitrogen rejection.[33,34] The size and location of each processing plant are usually the most important design decisions due to their high capital investment. Through this shale gas processing, compounds and gases, oil, and water mixed with the natural gas are removed, and two major products, the "pipeline-quality" sales gas and NGLs, are extracted and sold separately.

The downstream of shale gas supply chain mainly involves the storage, distribution, and sale of natural gas. According to the U.S. EIA, there are four major natural gas customers, including electric power plants, industrial customers, commercial customers, and residential customers.[35] As their names indicate, in electric power plants, natural gas is used for power

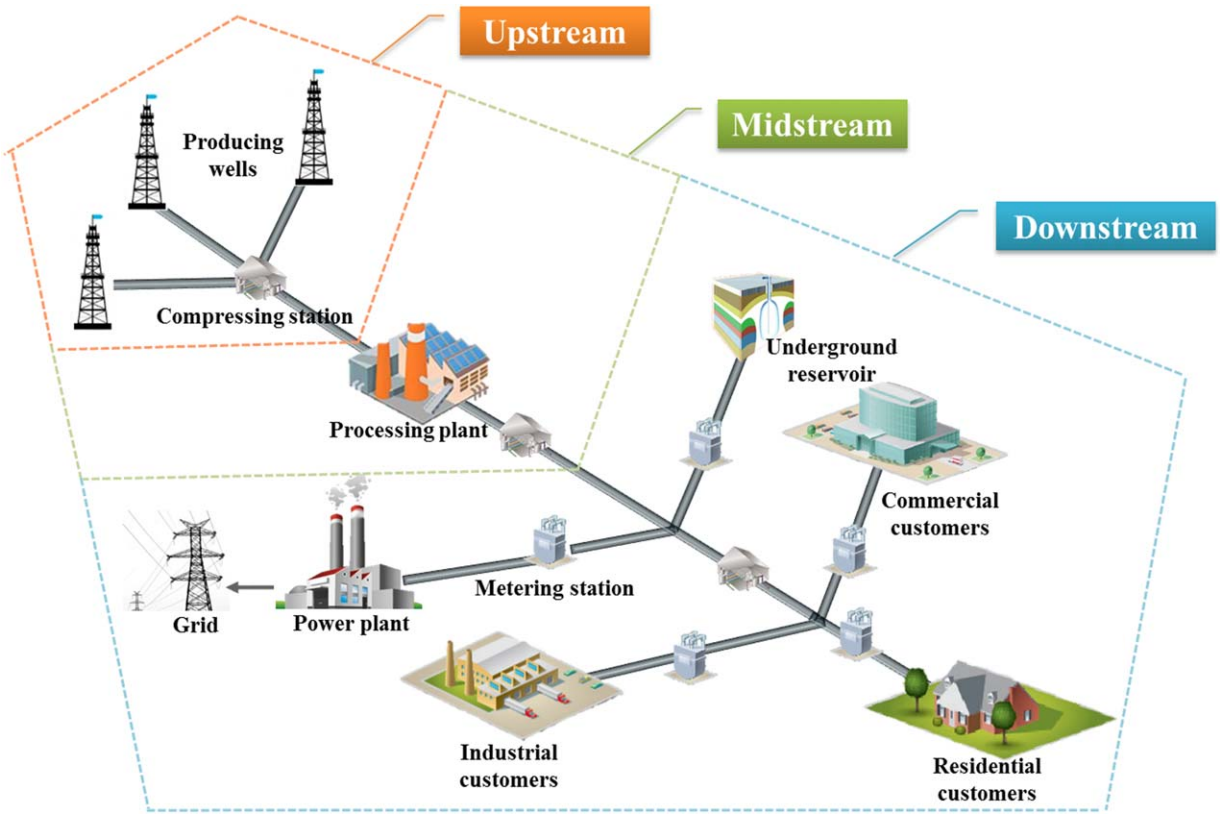

Figure 1. Overview of shale gas supply chain network.

[Color figure can be viewed in the online issue, which is available at wileyonlinelibrary.com.]

generation to supply electricity to the public. For industrial customers, natural gas is used for heat, power, or as a chemical feedstock by manufacturing establishments or those engaged in mining or other mineral extraction, as well as consumers in agriculture, forestry, and fisheries. For commercial customers, natural gas is used by nonmanufacturing establishments or agencies primarily engaged in the sale of goods or services. Residential customers use natural gas in private dwellings. Alternatively, natural gas can be transported to underground reservoirs for temporary storage. There are three principle types of underground storage sites in the U.S., namely, depleted natural gas or oil fields, aquifers, and salt caverns.[36] These underground reservoirs behave as a "buffer" in the shale gas supply chain to accommodate fluctuations in demand and price. Natural gas is mainly transported through pipeline networks. Depending on their exact function, there can be different sizes of pipelines ranging from 6 in. to 48 in. in diameter.[7] In the natural gas pipeline network, there are compressor stations and metering stations to provide necessary pressurization and measurement for the gas flow. Considering the significant capital investment for shale gas infrastructure, it is crucial to determine the optimal network design and operations decisions for the shale gas supply chain that can help to achieve the best economic performance especially under the uncertainty of shale well EUR.

Problem Statement

In this section, we formally state the problem of optimal design and operations of a shale gas supply chain under uncertainty. A superstructure of the shale gas supply chain network taken as a reference in this study is depicted in Figure 2.

As can be seen, such a network includes a set of shale sites with potential wells that can be drilled, a set of processing plants where sales gas and NGLs are separated, and a set of end customers, namely power plants, industrial customers, commercial customers, and residential customers, where natural gas is consumed to provide energy. Following existing literature, the storage option is neglected in this shale gas supply chain to simplify the complex network,[15] although the proposed modeling framework and solution algorithm are general enough to be easily adapted to consider this issue. Shale gas is transported through pipelines that need to be designed with appropriate capacity. In this problem, we are given the following parameters:

- Reference capital investment data regarding well drilling, construction of processing plants, and installation of gas pipelines;
- Operating costs with respect to hydraulic fracturing, shale gas production, shale gas processing, and transportation;
- Reference capacity data related to potential processing plants and pipelines;
- Problem specific data, including the reference production profile of shale gas, EUR sampling data of shale well, maximum number of wells that can be drilled for each shale site, composition of shale gas, processing efficiency at processing plants, sale price of NGL, minimum demand of natural gas, and average energy generation efficiency for different end customers.

Corresponding to the two-stage stochastic programming method, major decision variables comprise two stages. The first-stage decisions correspond to all the design decisions, which are made "here-and-now" prior to the realization of EUR uncertainty. The second-stage decisions are all the

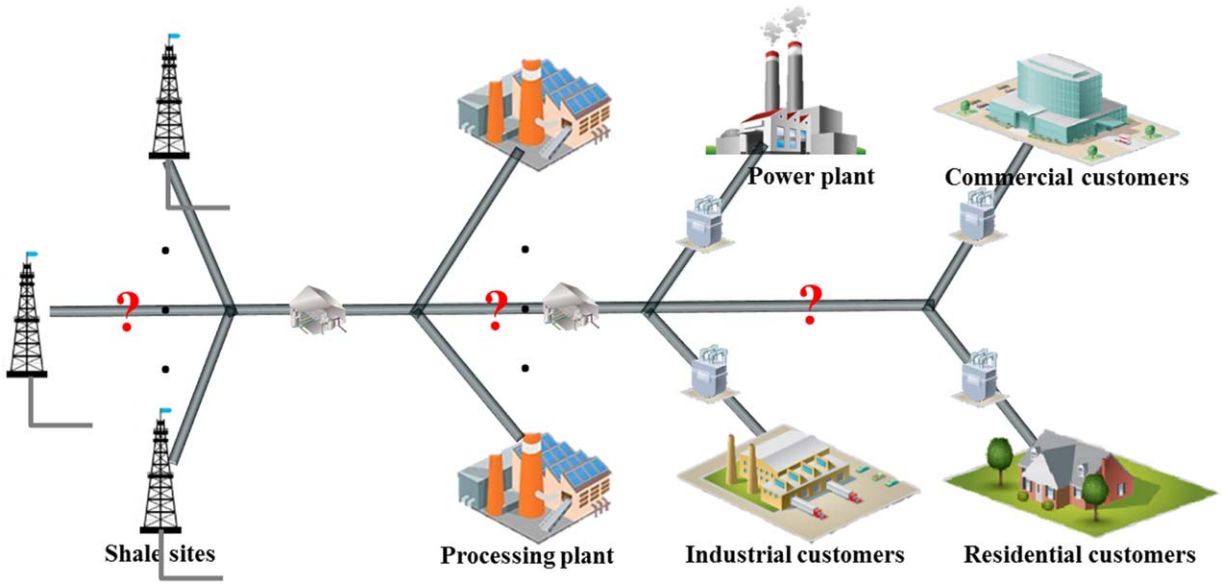

Figure 2. Superstructure of shale gas supply chain network.

[Color figure can be viewed in the online issue, which is available at wileyonlinelibrary.com.]

operational decisions that are postponed to a "wait-and-see" mode after EUR uncertainty and the shale gas production profile is revealed. Details of these decisions variables are given as the following:

Stage I: Design Decisions

- Number of wells to be drilled in each shale site;
- Constructions of processing plants and corresponding capacities;
- Installation and corresponding capacities of pipelines between shale sites, processing plants, and end customers.

Stage II: Operational Decisions

- Amount of shale gas produced at each shale site in each time period;
- Amount of shale gas processed at each processing plant in each time period;
- Amount of gas being sent to each end customer in each time period;
- Amount of energy generated corresponding to different end-use.

In this work, we make the following assumptions:

- Maximum number of wells that can be drilled at each shale site is known beforehand;
- Shale wells within the same shale site is lumped together in the supply chain;
- The total operational cost regarding all the activities related to shale gas production, such as hydraulic fracturing, pumping, water management, and so forth, is proportional to the amount of shale gas produced;
- NGL is known to have higher unit economic value than methane. Yet, NGL is considered as by-product of shale gas and sold at processing plants, because we focus on shale gas supply chain in this work;
- Minimum demand of natural gas for different end customer is estimated based on the overall scale of shale gas supply chain considered in this work.

The objective of this two-stage stochastic programming problem is to optimize the expected LCOE generated from Shale gas, which is formulated as minimizing the total expected cost of shale gas supply chain divided by the total energy generation.[37] The LCOE can be regarded as the cost at which electricity must be generated to break-even over the lifetime of the project.[38] Therefore, it is considered as an ideal economic indicator in a shale gas supply chain.[18] As a result, the goal of this model is to seek the best average economic performance of shale gas for energy generation under uncertainties of EUR of shale sites. It is also worth noting that currently, the noncooperative supply chain optimization problem is still very challenging to tackle. In this work, we assume a cooperative model in this work following the pattern of most existing supply chain optimization work.

Model Formulation

According to the general problem statement in the previous section, we present the model formulation for the optimal design and operations of shale gas supply chain networks. A list of indices, sets, parameters, and variables is given in the nomenclature, where all of the parameters are denoted with lower-case symbols, and all of the variables are denoted with upper-case symbols. A general description of the mathematical model is given as follows:

$$\text{Objective: min } \mathrm{E(LCOE)} = \frac{\mathrm{TC}}{\mathrm{TEG}} = \frac{\mathrm{TC_{1st}} + \sum_{js \in JS} \mathrm{TC_{2nd},}_{js} \cdot p_{js}}{\sum_{js \in JS} \mathrm{TEG_{2nd},}_{js} \cdot p_{js}}$$

s.t. Mass-balance constraints (11)–(15)
Capacity constraints (16)–(20)
Bounding constraints (21)–(23)
Logic constraints (24)–(28)

Objective function

The objective of this stochastic programming model is to optimize the expected LCOE, which is formulated as total expected net present cost (TC) divided by total expected

energy generation (TEG). The numerator TC equals the sum of the first-stage cost (TC_{1st}) and the expected second-stage cost. TC_{1st} accounts for the total capital investment, including the capital cost of shale well drilling and completion, installation of pipelines, and construction of processing plants. The expected second-stage cost is the summation of the products of the scenario probability p_{js} and the associated scenario cost $TC_{2nd,js}$. As we consider NGLs as by-products of sales gas, there are negative terms accounting for the extra income from selling NGLs. Positive terms include costs related to shale gas production operations, shale gas processing, and gas transportation. The denominator is the product of the scenario probability p_{js} and the associated scenario energy generation $TEG_{2nd,js}$.

The first-stage cost refers to total capital investment at the beginning of the planning horizon, calculated by

$$TC_{1st} = C_{1st}^{drilling} + C_{1st}^{processing} + C_{1st}^{pipeline} \tag{1}$$

where $C_{1st}^{drilling}$ is the capital investment of shale well drilling and completion. $C_{1st}^{processing}$ is the capital investment for construction of processing plants, and $C_{1st}^{pipeline}$ is the capital investment of pipeline networks that connect shale sites, processing plants, and end customers of natural gas. The first term is calculated by

$$C_{1st}^{drilling} = \sum_{i\in I} sdc_i \cdot NN_i \tag{2}$$

where NN_i is an integer variable that denotes the number of wells to be drilled at shale site i; sdc_i denotes the capital cost for shale well drilling and completion at shale site i;

The second term is given by

$$C_{1st}^{processing} = \sum_{p\in P}\sum_{r\in R}\left(\mathrm{pri}_{r-1}\cdot \mathrm{YP}_{p,r} + \left(\mathrm{PC}_{p,r} - \mathrm{prc}_{r-1}\cdot \mathrm{YP}_{p,r}\right)\cdot\left(\frac{\mathrm{pri}_r - \mathrm{pri}_{r-1}}{\mathrm{prc}_r - \mathrm{prc}_{r-1}}\right)\right) \tag{3}$$

where $PC_{p,r}$ denotes the processing capacity for range r processing plant p; YP_p is binary variable that equals 1 if processing plant p is constructed; pri_r is the reference capital investment for processing plant with capacity range r; and prc_r is the corresponding reference capacity for processing plant with capacity range r.

The last term is modeled as follows

$$C_{1st}^{pipeline} = \sum_{i\in I}\sum_{p\in P}\sum_{r\in R}\left(\mathrm{tpri}_{r-1}\cdot \mathrm{XP}_{i,p,r} + \left(\mathrm{TPC}_{i,p,r} - \mathrm{tprc}_{r-1}\cdot \mathrm{XP}_{i,p,r}\right)\cdot\left(\frac{\mathrm{tpri}_r - \mathrm{tpri}_{r-1}}{\mathrm{tprc}_r - \mathrm{tprc}_{r-1}}\right)\right) + \sum_{p\in P}\sum_{m\in M}\sum_{r\in R}\left(\mathrm{tpri}_{r-1}\cdot \mathrm{XPM}_{p,m,r} + \left(\mathrm{TPMC}_{p,m,r} - \mathrm{tprc}_{r-1}\cdot \mathrm{XPM}_{p,m,r}\right)\cdot\left(\frac{\mathrm{tpri}_r - \mathrm{tpri}_{r-1}}{\mathrm{tprc}_r - \mathrm{tprc}_{r-1}}\right)\right) \tag{4}$$

where $TPC_{i,p,r}$ denotes the transportation capacity of a range r pipeline from shale site i to processing plant p; $TPMC_{p,m,r}$ denotes the transportation capacity of a range r pipeline from processing plant p to end customer m; $XP_{i,p,r}$ is a binary variable that equals 1 if a pipeline is installed to transport shale gas from shale site i to processing plant p; $XPM_{p,m,r}$ is a similar binary variable indicating the construction of a pipeline transporting natural gas from processing plant p to end customer m; $tpri_r$ is the reference capital investment of a pipeline within capacity range r for transporting gases; and $tprc_r$ is the corresponding reference capacity of a pipeline within capacity range r.

The second-stage cost equals the summation of expected costs for shale gas production, shale gas processing, and gas transportation, subtracted by the expected income from sales of NGLs, given as

$$TC_{2nd,js} = C_{2nd,js}^{production} + C_{2nd,js}^{processing} + C_{2nd,js}^{transportation} - I_{2nd,js}^{NGLs} \tag{5}$$

$C_{2nd,js}^{production}$ refers to the operating costs in shale gas production that is proportional to the amount of shale gas produced, calculated by

$$C_{2nd,js}^{production} = \sum_{i\in I}\sum_{t\in T}\frac{\mathrm{spc}_{i,t}\cdot \mathrm{SP}_{i,t,js}}{(1+dr)^t} \tag{6}$$

where $SP_{i,t,js}$ is the shale gas production rate at shale site i in time period t in scenario js; $spc_{i,t}$ is the unit cost for shale gas production at shale site i in time period t; dr is the discount rate per time period.

$C_{2nd,js}^{processing}$ refers to the operating costs in processing plants that is proportional to the amount of shale gas processed, given by

$$C_{2nd,js}^{processing} = \sum_{i\in I}\sum_{p\in P}\sum_{t\in T}\frac{vp\cdot \mathrm{STP}_{i,p,t,js}}{(1+dr)^t} \tag{7}$$

where $STP_{i,p,t,js}$ denotes amount of shale gas transported from shale site i to processing plant p in time period t in scenario js; vp is the unit processing cost for shale gas.

$C_{2nd,js}^{transportation}$ indicates the total transportation cost, including the transportation of shale gas from shale sites to processing plants and transportation of sales gas between processing plants and different end customers

$$C_{2nd,js}^{transportation} = \sum_{i\in I}\sum_{p\in P}\sum_{t\in T}\frac{\mathrm{vtcs}\cdot \mathrm{lsp}_{i,p}\cdot \mathrm{STP}_{i,p,t,js}}{(1+dr)^t} + \sum_{p\in P}\sum_{m\in M}\sum_{t\in T}\frac{\mathrm{vtcm}\cdot \mathrm{lpm}_{p,m}\cdot \mathrm{STPM}_{p,m,t,js}}{(1+dr)^t} \tag{8}$$

where $STPM_{p,m,t,js}$ denotes the amount of natural gas transported from processing plant p to end customer m in time period t in scenario js; vtcs and vtcm indicate unit variable transportation costs for pipeline transportation of shale gas and sales gas, respectively; $lsp_{i,p}$ and $lpm_{p,m}$ indicate the distance from shale site i to processing plant p and the distance from processing plant p to end customers m, respectively.

$I_{2nd,js}^{NGLs}$ denotes the income of selling NGL at processing plants, calculated by

$$I_{2nd,js}^{NGLs} = \sum_{p\in P}\sum_{t\in T}\frac{\mathrm{pl}_t\cdot \mathrm{PLS}_{p,t,js}}{(1+dr)^t} \tag{9}$$

where $PLS_{p,t,js}$ denotes the amount of NGL sold at processing plant p in time period t in scenario js; pl_t denotes the average unit price of NGL in time period t.

The total energy generation $TEG_{2nd,js}$ corresponding to scenario *js* equals the summation of energy generated from different end customers, including the electric power consumption, industrial consumption, commercial consumption, and residential consumption, calculated by

$$TEG_{2nd,js}=\sum_{m\in M}\sum_{t\in T}\sum_{js\in JS} ue_m \cdot ect \cdot \sum_{p\in P} STPM_{p,m,t,js} \quad (10)$$

where ue_m denotes the average energy utilizing efficiency at end customer *m*; ect is the energy content of natural gas.

Constraints

Mass-Balance Constraints. The total shale gas production rate at a shale site equals the sum of the individual production rates of the different wells. Therefore, the total shale gas production at each shale site in each time period can be calculated by

$$SP_{i,t,js}=NN_i \cdot spp_{i,t} \cdot eur_{i,js},\ \forall i,\ t,\ js \quad (11)$$

where $spp_{i,t}$ denotes the shale gas production profile of a shale well at shale site *i* in time period *t*; we use this time-dependent parameter to account for the decreasing feature of the shale gas production profile of a certain well.[15,18] $eur_{i,js}$ is the parameter accounting for different EURs of the shale well at shale site *i* in scenario *js*.

The total amount of shale gas production at each shale site is equal to the total amount of shale gas transported to different processing plants

$$SP_{i,t,js}=\sum_{p\in P} STP_{i,p,t,js},\ \forall i,\ t,\ js \quad (12)$$

The total methane produced at a processing plant is equal to the methane composition of the total shale gas transported from different shale sites taking into account processing efficiency. The amount of NGLs produced at a processing plant is determined by similar equations

$$\sum_{i\in I} STP_{i,p,t,js} \cdot pef \cdot mc_i=SPM_{p,t,js},\ \forall p,\ t,\ js \quad (13)$$

$$\sum_{i\in I} STP_{i,p,t,js} \cdot pef \cdot lc_i=SPL_{p,t,js},\ \forall p,\ t,\ js \quad (14)$$

where $SPM_{p,t,js}$ is the amount of natural gas produced at processing plant *p* in time period *t* in scenario *js*; pef is the processing efficiency in terms of raw shale gas; mc_i denotes the average methane composition in shale gas at shale site *i*; $SPL_{p,t,js}$ stands for the amount of NGLs produced at processing plant *p* in time period *t* in scenario *js*; lc_i is the average NGL composition in shale gas at site *i*.

The total amount of natural gas produced at a processing plant is equal to the sum of natural gas transported from the processing plant to different end customers

$$SPM_{p,t,js}=\sum_{m\in M} STPM_{p,m,t,js},\ \forall p,\ t,\ js \quad (15)$$

Capacity Constraints. The amount of shale gas transported by pipeline from shale site *i* to processing plant *p* is bounded by the capacity of pipelines, given by

$$STP_{i,p,t,js} \le \sum_{r\in R} TPC_{i,p,r},\ \forall i,\ p,\ t,js \quad (16)$$

The amount of natural gas transported by pipeline from processing plant *p* to end customer *m* is bounded by the capacity of pipelines, given by the following constraints

$$STPM_{p,m,t,js} \le \sum_{r\in R} TPMC_{p,m,r},\ \forall p,\ m,\ t,\ js \quad (17)$$

The total amount of shale gas from all the shale sites processed by each processing plant should not exceed its processing capacity

$$\sum_{i\in I} STP_{i,p,t,js} \le \sum_{r\in R} PC_{p,r},\ \forall p,\ t,\ js \quad (18)$$

The total amount of natural gas transported from all the processing plants to each end customer should meet their minimum demands

$$dm_{m,t} \le \sum_{p\in P} STPM_{p,m,t,js},\ \forall m,\ t,\ js \quad (19)$$

where $dm_{m,t}$ denotes the minimum demand of natural gas at demand node *m* in time period *t*.

Similarly, the total amount of NGLs sold at all the processing plants is also bounded below by its minimum demand, given as

$$dl_t \le \sum_{p\in P} PLS_{p,t,js},\ \forall t,\ js \quad (20)$$

where dl_t denotes the minimum demand for NGLs in time period *t*.

Bounding Constraints. The constraints for the capacity of pipeline transporting shale gas from shale site *i* to processing plant *p* are given by

$$tprc_{r-1} \cdot XP_{i,p,r} \le TPC_{i,p,r} \le tprc_r \cdot XP_{i,p,r},\ \forall i,\ p,\ r\ge 2 \quad (21)$$

Similarly, the constraints for the capacity of pipelines transporting natural gas are given by

$$\begin{aligned} tprc_{r-1} \cdot XPM_{p,m,r} &\le TPMC_{p,m,r} \\ &\le tprc_r \cdot XPM_{p,m,r},\ \forall p,\ m,\ r\ge 2 \end{aligned} \quad (22)$$

If a processing plant is established, its processing capacity should be bounded by the corresponding capacity range; otherwise, its capacity should be zero. This relationship can be modeled by the following inequality

$$prc_{r-1} \cdot YP_{p,r} \le PC_{p,r} \le prc_r \cdot YP_{p,r},\ \forall p,\ r\ge 2 \quad (23)$$

Logic Constraints. For the drilling issue of the shale well, we have the following logic constraints.

The total number of wells drilled all shale sites should satisfy the following constraint

$$\sum_{i\in I} NN_i \ge tln,\ \forall i \quad (24)$$

where tln denotes the minimum total number of wells that are planned to be drilled in this project.

The total number of wells that can be drilled at shale site *i* over the planning horizon is bounded by

$$NN_i \le tmn_i,\ \forall i \quad (25)$$

where tmn_i denotes the maximum number of wells that can be drilled at shale site *i*.

For all the pipelines in this supply chain, we assume only one capacity range *r* can be chosen

$$\sum_{r\in R} XP_{i,p,r} \le 1,\ \forall i,\ p \quad (26)$$

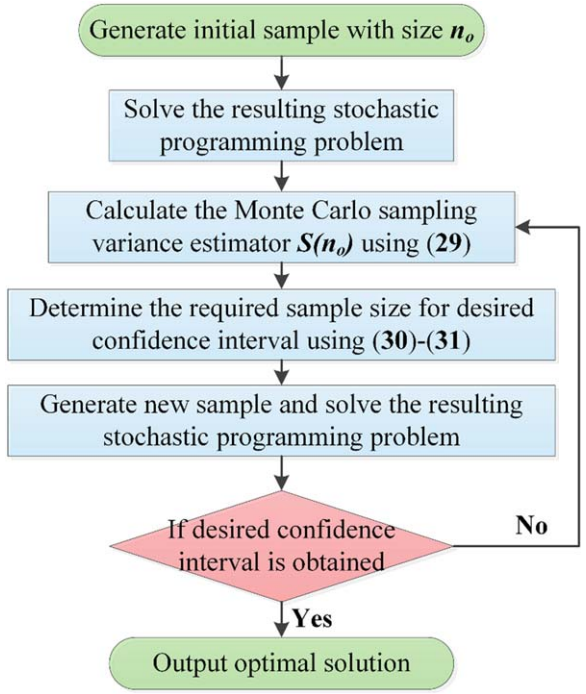

Figure 3. Flowchart on determining the sample size.

[Color figure can be viewed in the online issue, which is available at wileyonlinelibrary.com.]

$$\sum_{r\in R} \mathrm{XPM}_{p,m,r} \le 1,\ \forall p,\ m \tag{27}$$

Similarly, only one capacity range r can be selected for all processing plants

$$\sum_{r\in R} \mathrm{YP}_{p,r} \le 1,\ \forall p \tag{28}$$

Solution Approaches

Scenario-based stochastic programming models are often computationally demanding, because their model size will increase exponentially as the number of scenarios increases.[39] In this shale gas supply chain model, if we only consider three shale sites in total and 100 independent EUR scenarios for each of them, then there will be $100^3 = 1{,}000{,}000$ scenarios in total. Moreover, the resulting problem is a large-scale two-stage SMILFP problem, which is known to be computationally challenging due to its combinatorial natural and pseudoconvexity.[40,41] Considering the complexity of this shale gas supply chain model, it is necessary to develop solution strategies to circumvent these computational challenges and improve solution efficiency.

SAA method

In this work, we consider a SAA approach for the two-stage stochastic programming problem.[29,42] As a common approach to reduce a scenario set to a manageable size, the basic idea of this approach is to generate a sample of the uncertain parameter (normally the parameters are assumed to be independent identically distributed) to approximate the original expected objective value by calculating the sample average. We use Monte Carlo methods to generate scenarios based on existing EUR data of 2600 shale wells as reported in the Marcellus shale play.[22,31] Oracle Crystal Ball[43] software is applied as the sample generator.

In the SAA approach, the number of scenarios is determined by the desired level of solution accuracy, which can be measured by the confidence interval of the optimal solution. A well-controlled choice of the sample can significantly reduce the computational time and improve the accuracy of optimal solutions. In this work, we determine the proper sample size following the framework given in Figure 3.

As can be seen in Figure 3, to determine the "optimal" number of scenarios N^*, we first solve the stochastic programming problem with a small initial sample size n_0 (e.g., 10–100). Based on the optimal solutions obtained, we can then calculate the Monte Carlo sampling variance estimator $S(n_0)$ using the following equation

$$S(n_0) = \sqrt{\frac{\sum_{s=1}^{n_0} (\mathrm{E(LCOE)} - \mathrm{LCOE}_s)^2}{n_0 - 1}} \tag{29}$$

where LCOE, as mentioned before, is the levelized cost of energy generated from shale gas, that is, our objective value, and LCOE_s corresponds to scenario s. Based on this sampling variance estimator, we are able to calculate the confidence interval of $1-\alpha$, given as

$$\left[\mathrm{E(LCOE)} - \frac{z_{a/2} S(n_0)}{\sqrt{n_0}}, \mathrm{E(LCOE)} + \frac{z_{a/2} S(n_0)}{\sqrt{n_0}}\right] \tag{30}$$

where $z_{\alpha/2}$ is the standard normal deviation such that $1-\alpha/2$ satisfies a standard normal distributed variable $z \sim N(0,1)$, $Pr(z \le z_{\alpha/2}) = 1-\alpha/2$. For example, if we consider a 98% confidence interval ($1-\alpha = 98\%$), then $z_{\alpha/2} = 2.06$.

Given the sampling variance estimator $S(n_0)$ and the desired confidence interval H, we can calculate the minimum number of required scenarios by the following equation

$$N^* = \left[\frac{z_{\alpha/2} S(n_0)}{H}\right]^2 \tag{31}$$

Based on the minimum number of scenarios obtained above, we update the sample size and then solve the new stochastic programming problem again following the same strategy. A verifying step is added to make sure the required confidence interval is achieved after solving the updated stochastic programming problem. If this stopping criterion is satisfied, the corresponding optimal solution is taken as a good approximation of the exact optimal solution of the original stochastic programming problem.[30]

In this work, by setting an initial sample size of 100 scenarios and considering a 98% confidence interval, we finalize the required number of scenarios as 300. In Figure 4, a comparison between the exact EUR distribution data derived from literature[22] and that from sample approximation is presented.

As can be seen, the SAA approach provides an excellent approximation of the original EUR distribution. In addition, suppose we consider 100 discrete EUR scenarios for each of the 10 shale sites, the total number of scenarios would be 100^{10} ($\sim 10^{20}$). By applying the SAA technique, a sample size of around 300 is enough to find the optimal solution with 98% possibility. However, we note that the resulting stochastic program is still a large-scale two-stage SMILFP problem that can be challenging to solve. In the following section, we introduce

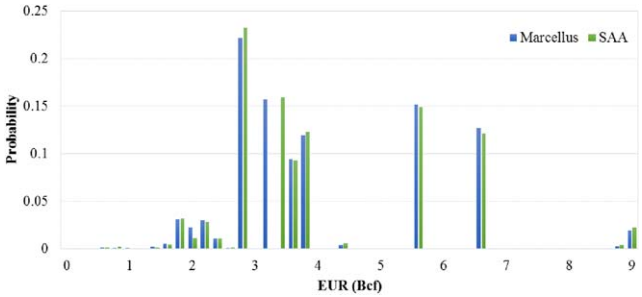

Figure 4. Comparison of EUR distribution between exact data for Marcellus derived from literature and data from SAA.

[Color figure can be viewed in the online issue, which is available at wileyonlinelibrary.com.]

a novel algorithm taking advantage of the special structure of the problem to tackle the resulting SMILFP problem.

A novel optimization algorithm

SMILFP is a specially class of MINLP that includes both fractional objective resulting from MILFP and L-shaped constraints due to the stochastic programming formulation. The large-scale two-stage stochastic programming problem is difficult to solve.[39] Moreover, it is known that global optimization of MILFP problems can be computationally intractable because of their combinatorial nature and pseudoconvexity.[44–46] Consequently, as a combination of these two types of challenging optimization problems, the resulting two-stage SMILFP problem is not expected to be solved efficiently by any off-the-shelf solvers. By exploiting the problem structure, we propose a novel and efficient optimization algorithm that combines the parametric approach as well as the L-shaped method as an effective way to tackle this difficult problem. In this work, we first apply the parametric algorithm based on the exact Newton's method to circumvent the computational challenge resulting from the fractional objective function.[47–49] As a result, a parameter uc is introduced to replace the fractional objective function with a linear parametric function, and the original SMILFP problem is transformed to a set of stochastic mixed-integer linear programming (SMILP) subproblems targeting on finding the optimal value of uc. To further improve the computational efficiency, the resulting two-stage SMILP subproblem is solved using the L-shaped method.[50,51] To provide a comprehensive idea of this algorithm, a flowchart of this novel solution algorithm is given at first. Afterwards, we present the general-form model formulation and solution strategies. At last, a pseudocode of this novel solution algorithm is provided. The detailed model formulations of dual-subproblems and the corresponding cutting planes are included in Appendix B.

The whole solution algorithm is summarized in Figure 5. As can be seen, this solution algorithm integrates the parametric algorithm and the L-shaped method through the inner and outer loops. In the outer loop, we apply the parametric algorithm to transform the original SMILFP problem to an equivalent parametric SMILP problem. In the inner loop, L-shaped method is used to tackle the two-stage SMILP problem. Based on the solution of each subproblem corresponding to different scenarios considered, we are able to updates either optimality cuts or feasibility cuts to the master problem, thus updating the LB and UB in the inner loop. Once the inner loop converges, the parameter uc can be updated, which leads to the next outer iteration.

Next, we consider a general form of the SMILFP model formulation (**P0**) to illustrate this solution approach in detail

$$(\mathbf{P0}) \rightarrow \min_{x,y_s} \frac{c^T x + \sum_{s\in S} p_s q_s^T y_s}{\sum_{s\in S} p_s r_s^T y_s} \tag{32}$$

$$\text{s.t. } Ax = b,\ x \geq 0 \tag{33}$$

$$Wy_s = h_s - T_s x,\ y_s \geq 0,\ s \in S \tag{34}$$

First, by applying parametric algorithm, (**P0**) can be transformed into the following parametric form (**P1**)

$$(\mathbf{P1}) \rightarrow \min_{x,y_s} F(uc) = c^T x + \sum_{s\in S} p_s q_s^T y_s - uc \cdot \sum_{s\in S} p_s r_s^T y_s \tag{35}$$

$$\text{s.t. } Ax = b,\ x \geq 0 \tag{36}$$

$$Wy_s = h_s - T_s x,\ y_s \geq 0,\ s \in S \tag{37}$$

then the target is to find a parameter uc such that $F(uc) = 0$.[47] As $F(uc)$ does not have a closed-form analytical expression, we can apply a numerical root finding method, namely the exact Newton's method, to solve the subproblem and update the parameter uc.[47]

Because (**P1**) is an SMILP problem, we can apply the well-known L-shaped method and solve the resulting two-stage SMILP.[52,53] The corresponding master problem and subproblem are given as follows:

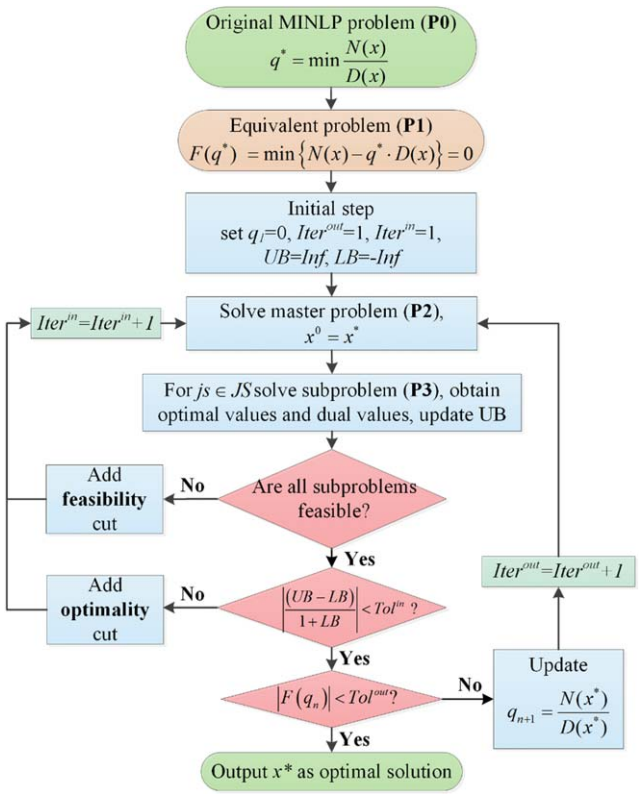

Figure 5. Flowchart of the solution algorithm integrating parametric approach and L-shaped method.

[Color figure can be viewed in the online issue, which is available at wileyonlinelibrary.com.]

Global Optimization Algorithm

$uc \leftarrow 0$, $Iter^{out} \leftarrow 1$,
while ($F(uc) \geq Tol^{out}$) **do**
  $Iter^{out} \leftarrow Iter^{out}+1$
  $LB \leftarrow -\infty$, $UB \leftarrow +\infty$, $Iter^{in} \leftarrow 1$, $Gap \leftarrow +\infty$
  Solve (**P2**) to obtain initial first-stage decisions
  while ($Gap \geq Tol^{in}$) **do**
    $Iter^{in} \leftarrow Iter^{in}+1$
    while (*terminate* =**false**) **do**
      Scenario $s \leftarrow s+1$
      Solve (**P3**) with given first-stage decisions
      if ((**P3**) of scenario s is feasible) **then**
        Generate optimality cut: $\theta \geq e_o x + d_o$
      else
        Generate feasibility cut: $e_f x + d_f \leq 0$
      end if
      if $count(s) \geq |S|$ **then**
        $terminate \leftarrow$ **true**
      end if
    end while
    if (all the (**P3**) are feasible) **then**
      Add $\theta \geq e_o x + d_o$ to (**P2**), update UB
    else
      Add $e_f x + d_f \leq 0$ to (**P2**)
    end if
    Solve (**P2**) with updated cuts
    Update LB
  end while
  Update parameter uc
end while
Output uc^* as global optimal value

Figure 6. Pseudocode of the global optimization algorithm.

Master Problem:

$$(\mathbf{P2}) \rightarrow \min_{x,y_s} c^T x+\theta \tag{38}$$

$$\text{s.t. } Ax=b,\ x \geq 0 \tag{39}$$

$$\theta \geq e_o x+d_o,\ o=1...N \tag{40}$$

$$e_f x+d_f \leq 0,\ o=1...N' \tag{41}$$

Subproblem:

$$(\mathbf{P3}) \rightarrow \min_{x,y_s} F(uc)=\sum_{s\in S} p_s q_s^T y_s - uc \cdot \sum_{s\in S} p_s r_s^T y_s \tag{42}$$

$$\text{s.t. } Wy_s=h_s-T_s x,\ y_s \geq 0,\ s \in S \tag{43}$$

where the inequalities (40) and (41) in (**P2**) are "optimality cuts" and "feasibility cuts," respectively that link the master problem and the subproblem; e_o, d_o, e_f, and d_f are coefficients for the Benders cut, which can be calculated based on the solution to the corresponding subproblems. In each inner iteration of the L-shaped method, we first solve the master problem to obtain the initial first-stage decisions. These design decisions are then fixed in the solution of subproblems. Corresponding optimality cuts and feasibility cuts are generated following the above formulations. Depending on the solution of all the subproblems, we update the cut planes in the master problem and go to the next iteration. Detailed formulation of these equations is provided in Appendix B.

To better illustrate the proposed solution algorithm, a pseudocode is given in Figure 6.

Case Studies

To illustrate the applicability of the proposed model and solution strategy, one specific case study based on the Marcellus shale play is considered in this work. A detailed description of this problem is given below. It is worth noting that the proposed modeling framework and optimization algorithm are general enough, so their application is not limited to any specific case study region. Moreover, to illustrate the practicality of the proposed SMILFP model, we consider a traditional SMILP model that minimizes the total cost for comparison. The corresponding results are summarized in Appendix D.

In this case study, a total of 10 potential shale sites are considered, and each of them can drill up to four to eight shale wells at maximum.[54] All the drilling decisions are made at the beginning of the planning horizon. An exponentially decreasing approximation of the shale gas production profile is considered, which is a function of time and given in Appendix A.[15] There are three potential shale gas processing plants. Four types of end customers of shale gas are considered, including power plants, industrial customers, commercial customers, and residential customers. The capital investment of processing plants and pipelines are evaluated using a piecewise approximation approach, and four capacity ranges are considered with respect to corresponding design decisions. The total planning horizon is 10 years, which is close to the real lifetime of shale wells, and it is divided into 10 time periods (1 year per time period).[15,55] In this work, we adopt a 10% discount rate for each year.[56] All the detailed input data are based on existing literature and given in Appendix A. The resulting problem has 174,375 continuous variables (Stage I: 180; Stage II: 174,195), 190 discrete variables (Stage I: 190; Stage II: 0), and 249,421 (Stage I: 433; Stage II: 248,988) constraints. All of the models and solution procedures are coded in GAMS 24.4.1[57] on a PC with an Intel® Core™ i5-2400 CPU @ 3.10 GHz and 8.00 GB RAM, running Window 8, 64-bit operating system. Furthermore, the MILP problems are solved using CPLEX 12.6. The absolute optimality tolerance for all solvers is set to 10^{-6}. The optimality tolerance for the inner loop in the proposed global optimization method is set to 10^{-2}, and the optimality tolerance for the outer loop is set to 10^{-3}.

Computational results

As discussed in the solution approach section, we propose a novel global optimization algorithm to tackle this two-stage SMILFP problem, which integrates the parametric algorithm as well as the L-shaped method. By applying the parametric algorithm, we are able to circumvent the fractional-form objective and solve an MILP problem instead. In each iteration of the outer loop, the introduced parameter uc is updated. Meanwhile, the inner loop of this algorithm consists of the L-shaped method. Through a set of iterations between the master problem and subproblem, the lower bound and upper bound keep updating until the final stopping criterion is satisfied. In this work, we choose CPLEX as the MILP solver, and the initial value of uc is set to 0. We note that general-purpose global MINLP solvers, namely BARON and SBB, cannot return any feasible solution to this problem within 10 h, so we only present the computational results of the proposed solution algorithm. In Figure 7, we explicitly present the converging process of this algorithm as it solves the case study.

The total computational time is 1590 CPU sec, and there are a total of three outer loop iterations corresponding to the parametric algorithm. In the first outer loop iteration, the L-shaped method takes 17 inner iterations to converge. In the second outer loop iteration, where the parameter uc is updated, the L-shaped method takes 34 inner iterations to converge. In the third outer loop iteration, 95 inner iterations are required for the L-shaped method to converge to the optimal value of parameter uc^*, such that $F(uc^*)$ is smaller than the optimality

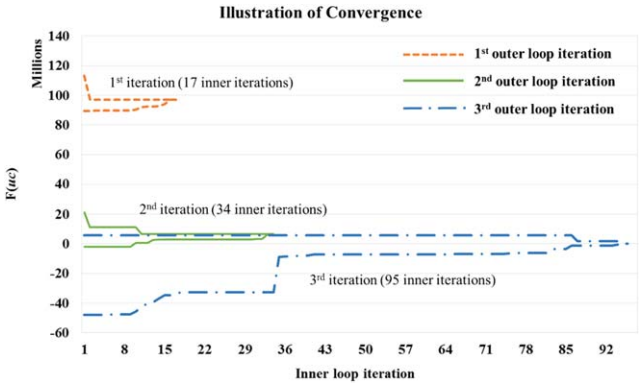

Figure 7. Converging process of the proposed algorithm.

[Color figure can be viewed in the online issue, which is available at wileyonlinelibrary.com.]

tolerance. It is worth noting that as the value of the parametric objective function approaches the optimal value, more inner iterations are required to converge to the specified tolerance.

Optimization results

As can be seen in Figure 8, we present the optimal design of the shale gas supply chain under EUR uncertainty. The overall trend is to build a centralized supply chain network. Instead of drilling evenly in more shale sites with less shale wells for each site, only three shale sites, namely shale site 2, shale site 7, and shale site 10, are selected among the 10 potential shale sites as the optimal shale gas producers. A total of 12 shale wells are drilled, of which five wells are assigned to shale site 2, four wells are assigned to shale site 7, and three wells are assigned to shale site 10. By exploring the possible reasons, we find that: first, the chosen shale sites 2, 7, and 10 have relatively higher average EUR considering the given sample data. In addition, the distances between the aforementioned shale sites and processing plant 2, which is planned to be constructed, are relatively shorter. Therefore, we conclude that the final selection of these shale sites is a decision based on simultaneous considerations of both EUR and transportation factors. As a result, more shale gas is expected to be produced under a fixed drilling, fracturing, and completion cost. Moreover, the corresponding transportation investment as well as operating cost can be reduced to some extent. Similar to the drilling decisions, only one of the three potential shale gas processing plants is constructed with a large processing capacity, given as 22.8 Billion Standard Cubic Feet per year (Bscf/year). Although it might be possible to reduce the overall transportation cost by building more processing plants with smaller sizes considering the relative position of shale sites and processing plants, the overall capital investment of processing plants is expected to be greater due to the economies of scale, and more importantly, uncertain shale gas production for each shale site. To summarize, we conclude that a single, large size processing plant is a more reliable and economical choice under EUR uncertainty.

To illustrate the value of our stochastic programming model, we present the results of the Expected Value of Perfect Information (EVPI) and the Value of the Stochastic Solution (VSS).[52] The EVPI measures the maximum price a decision maker would be ready to pay in return for complete and accurate information about the future (i.e., the exact EUR data in this work). To calculate the EVPI, we solve each scenario in isolation and then compute the average of the individual optimal solutions. This value is known as the average performance in case of perfect information. The EVPI is defined as the difference between the average performance with perfect information and the optimal stochastic solution. Conversely, the VSS shows the superiority of the optimal stochastic solution over that of a single deterministic model with all uncertainties replaced by their expected values. To obtain the VSS, we solve the deterministic model where all EUR parameters are replaced by their expectations, and then we evaluate that solution (fixing all design decisions) against all the scenarios, and compute its average performance. The VSS is defined as the difference between the optimal stochastic solution and the average performance of the deterministic solution. The detailed results are given in Figure 9.

As shown in Figure 9, the orange line is the objective value obtained by solving the SMILFP problem, which is \$0.0038/MJ. The green dots indicate the exact objective values obtained with fixed design decisions from the deterministic model. Depending on the exact scenarios, the deviation can be significant, leading to the conclusion that EUR uncertainty

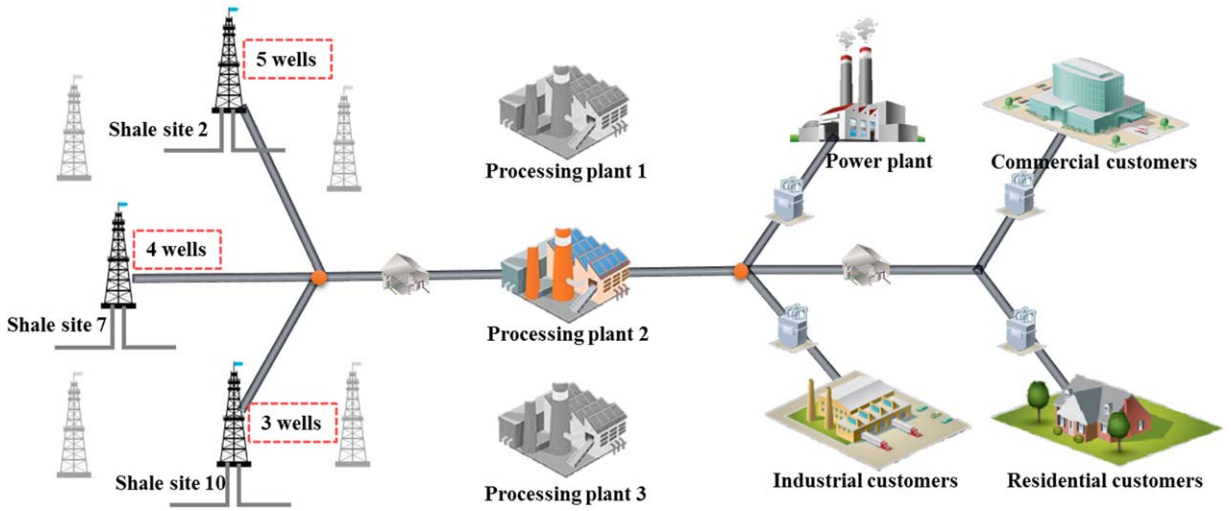

Figure 8. Optimal design of shale gas supply chain network under EUR uncertainty.

[Color figure can be viewed in the online issue, which is available at wileyonlinelibrary.com.]

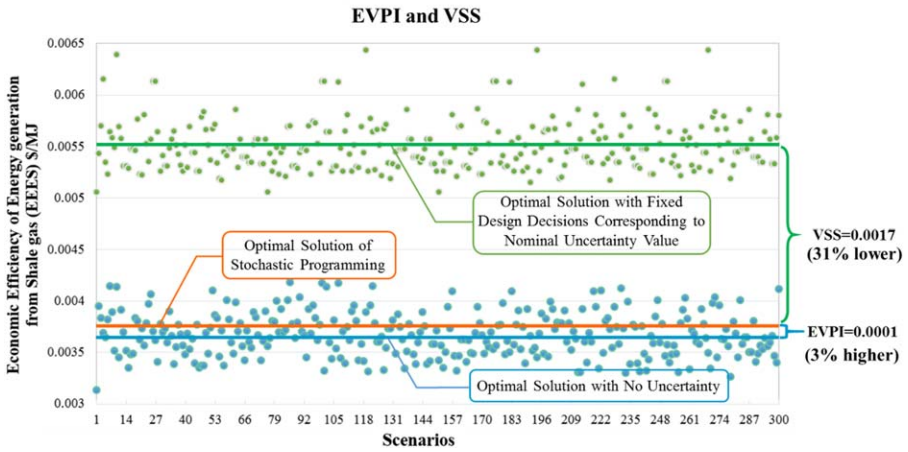

Figure 9. Results of EVPI and VSS with 300 scenarios considered.

[Color figure can be viewed in the online issue, which is available at wileyonlinelibrary.com.]

does pose great impacts on the final economic efficiency of a shale gas supply chain. The green line crossing these green dots shows the average performance of the deterministic model, which is $0.0055/MJ. Similarly, the blue dots are the objective values obtained with perfect information (no uncertainty) on EUR for all scenarios, and the corresponding blue line shows the average performance in case of perfect information, which is $0.0037/MJ. We notice a smaller spread of the blue dots compared with that of the green dots, which indicates that improper design decisions from deterministic models will exaggerate the impacts of uncertain EUR on economic performance. Based on these values, we calculate the EVPI and VSS as $0.0001/MJ and $0.0017/MJ, respectively. The stochastic programming model certainly shows great potential to improve the overall economic performance of shale gas supply chain over a deterministic one: the LCOE is improved by over 30%. Additionally, the stochastic programming model performs quite well even compared with the perfect information model, of which the LCOE is only 3% less.

In Figure 10, we rearrange the results of the green and blue dots to present the corresponding possibility distributions to better present the solutions from both the deterministic model and the model with perfect information. In addition, we present the drilling schedule and the supply chain design corresponding to the deterministic model for a better comparison, included in Appendix C.

From the comparison, we conclude that when EUR uncertainty are taken into account, the deterministic model based on nominal values will result in significant variance of economic performance depending on the exact realization of uncertainty, and the average economic performance is much worse than that of stochastic model (30% higher LCOE). Moreover, it is impressive to see that the stochastic model can provides an optimal solution whose average performance is very close to the ideal one with perfect information (3% lower LCOE). Therefore, it is proven to be of great importance to account for the EUR uncertainty when conducting shale gas supply chain optimization.

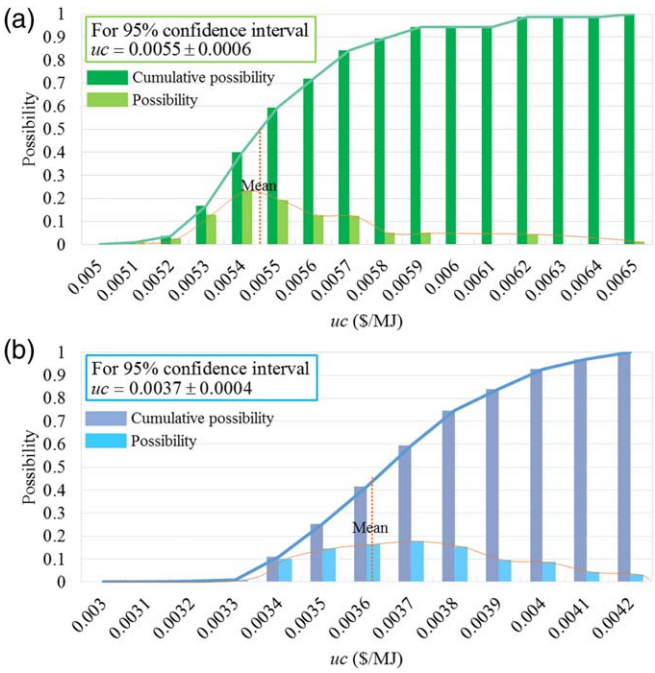

Figure 10. Possibility distribution of solutions from (a) deterministic model with nominal uncertainty value and (b) model with perfect information.

[Color figure can be viewed in the online issue, which is available at wileyonlinelibrary.com.]

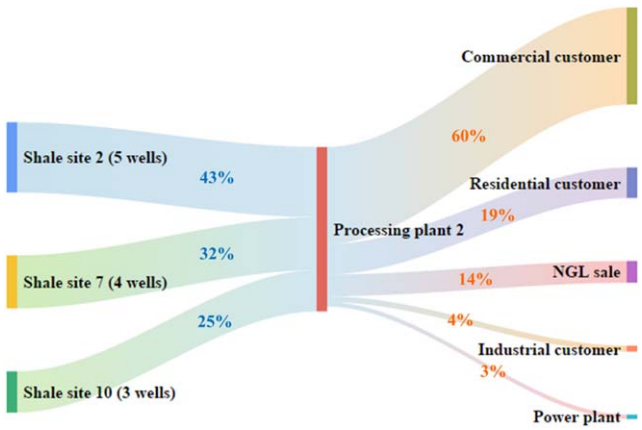

Figure 11. Sankey diagram of shale gas flow in the supply chain network.

[Color figure can be viewed in the online issue, which is available at wileyonlinelibrary.com.]

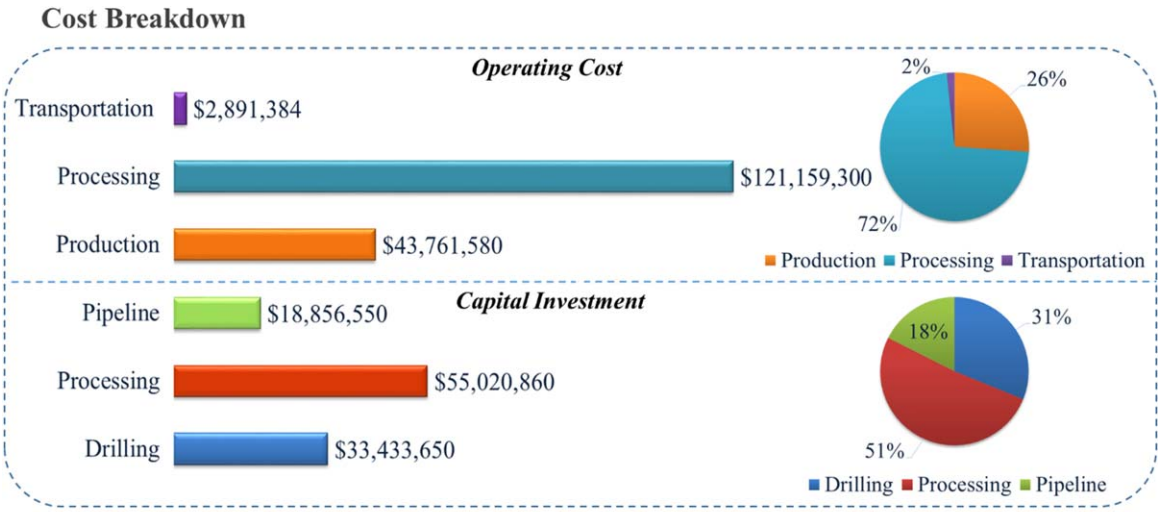

Figure 12. Cost breakdown regarding capital investment and operating cost.

[Color figure can be viewed in the online issue, which is available at wileyonlinelibrary.com.]

In the rest of this section, we focus on analyzing the optimal solutions obtained from the stochastic programming problem. One important concern is about the shale gas flow through the shale gas supply chain network. In Figure 11, we use a Sankey diagram to visualize the flow of shale gas within this shale gas supply chain network. As can be seen, with different shale wells drilled, shale sites 2, 7, and 10 produce different amounts of shale gas. Approximately 19.9 Bscf of shale gas is expected to be produced at shale site 2, 15.0 Bscf of shale gas is expected to be produced at shale site 7, and 11.7 Bscf at shale site 10. A total of 46.6 Bscf of shale gas is transported to processing plant 2 via pipeline. After being processed and separated, the sales gas is transported to different end customers, while NGLs are sold to nearby market. According to the optimal results, 3.2% of the natural gas is sent directly to power plants for electricity generation; 4.2% of the natural gas is transported to industrial customers; 70.4% of the natural gas is transported commercial customers, and 22.1% of the natural gas is sent to residential customers. The decision on the final distribution of natural gas involves comprehensive consideration of product transportation as well as the average energy generation efficiency corresponding to different end customers.

The overall cost distribution is summarized in Figure 12, in which the total expected cost is classified into two categories, namely capital investment and operating cost, and further analyzed corresponding to different processes within this shale gas supply chain. A total cost of $275.1 million is expected over this planning horizon, of which 61.0% is the operating cost, including $2.9 million spent on transportation, $121.1 million on shale gas processing, and $43.8 million on the shale gas production. The remaining 39% of the total cost is capital investment, of which $18.9 million is spent on pipeline installation, $55.0 million is contributed to construction of processing plants, and $33.4 million is for well drilling activities. The detailed cost breakdowns are given in the pie-charts as shown below. From this cost breakdown, we conclude that shale gas production and processing account for the major operating costs, and decisions on construction of processing plants and drilling activities lead to the greatest capital investment. Correspondingly, the variables related to these activities are expected to be the key drivers for operating cost and capital invest.

Conclusion

To the best of our knowledge, this is the first article that systematically addresses the optimal design and operations of shale gas supply chains under uncertainty. A scenario-based two-stage stochastic programming model was developed as a large-scale SMILFP problem. The objective was to optimize the LCOE generated from shale gas. All of the design decisions are made in the master problem, including drilling schedule, decisions on construction of processing plants, and corresponding pipeline designs. Meanwhile, recourse operating decisions are made in subproblems corresponding to different EUR sampling data, including the shale gas production, planning on shale gas processing, and distribution to end customers. To solve this computationally challenging problem efficiently, we applied the SAA method and proposed a novel algorithm integrating the parametric algorithm and the L-shaped method to take advantage of the model structure. One case study based on the Marcellus shale play was presented to illustrate the applicability of the proposed modeling framework and solution algorithm. The results indicated that the stochastic programming model was a superior choice for determining the optimal economic performance of a shale gas supply chain under EUR uncertainty. The shale gas production and processing activities account for the major operating costs, and decisions on construction of processing plants and drilling activities lead to the greatest capital investment. It is worth noting that the proposed model and solution approaches could be easily extended to consider other uncertainties, such as prices, demands, and property parameters. Moreover, instead of assuming a cooperative model, we may consider addressing the noncooperative case using game theoretical modeling approach,[58] which will be addressed in a future work.

Acknowledgment

The authors gratefully acknowledge the financial support from the Institute for Sustainability and Energy at Northwestern University (ISEN).

Notation

Sets

I = set of shale sites indexed by i
M = set of end customers indexed by m
P = set of processing plants indexed by p
T = set of time periods indexed by t
R = set of capacity levels indexed by r
JS = set of scenarios indexed by js

Parameters

dl_t = minimum demand for NGL in time period t
$dm_{m,t}$ = minimum demand of natural gas at end customer m in time period t
dr = discount rate per time period
ect = energy content of natural gas
$eur_{i,js}$ = parameter accounting for different EUR at shale site i in scenario js
lc_i = NGL composition in shale gas at shale site i
$lpm_{p,m}$ = distance from processing plant p to end customer m
$lsp_{i,p}$ = distance from shale site i to processing plant p
mc_i = methane composition in shale gas at shale site i
pef = processing efficiency of shale gas
pl_t = average unit price of NGL in time period t
prc_r = reference capacity for processing plant with capacity range r
pri_r = reference capital investment for processing plant with capacity range r
sdc_i = unit cost for shale well drilling and completion at shale site i in time period t
$spc_{i,t}$ = unit cost for shale gas production at shale site i in time period t
$spp_{i,\tau}$ = shale gas production of a shale well of age τ at shale site i
tln = minimum total number of wells to be drilled in this project
tmn_i = maximum number of wells that can be drilled at shale site i over the planning horizon
$tprc_r$ = reference capacity of pipeline with capacity range r transporting gases
$tpri_r$ = reference capital investment of pipeline with capacity range r transporting gases
ue = average energy utilizing efficiency at end customer m
vp = unit processing cost for shale gas
vtcm = unit variable transportation cost for pipeline transporting natural gas
vtcs = unit variable transportation cost for pipeline transporting shale gas

Continuous variables

$PC_{p,r}$ = processing capacity for range r processing plant p
$PLS_{p,t,js}$ = amount of NGL sold at processing plant p in time period t in scenario js
$SP_{i,t,js}$ = shale gas production rate at shale site i in time period t in scenario js
$SPL_{p,t,js}$ = amount of NGL produced at processing plant p in time period t in scenario js
$SPM_{p,t,js}$ = amount of natural gas produced at processing plant p in time period t in scenario js
$STP_{i,p,t,js}$ = amount of shale gas transported from shale site i to processing plant p in time period t in scenario js
$STPM_{p,m,t,js}$ = amount of natural gas transported from processing plant p to end customer m in time period t in scenario js
$TPC_{i,p,r}$ = transportation capacity of range r pipeline from shale site i to processing plant p
$TPMC_{p,m,r}$ = transportation capacity of range r pipeline from processing plant p to end customer m

Binary variables

$XP_{i,p}$ = 0–1 variable. Equal to 1 if pipeline is installed to transport shale gas from shale site i to processing plant p
$XPM_{p,m}$ = 0–1 variable. Equal to 1 if pipeline is installed to transport natural gas from processing plant p to end customer m
YP_p = 0–1 variable. Equal to 1 if processing plant p is constructed

Integer variables

NN_i = number of wells to be drilled at shale site i

Literature Cited

1. EIA. *Review of Emerging Resources: U.S. Shale Gas and Shale Oil Plays*. Washington, DC: U. S. Energy Information Administration, 2011.
2. EIA. *Annual Energy Outlook 2015 with Projections to 2040*. Washington, DC: U.S. Energy Information Administration, 2015.
3. Hughes JD. *Drilling Deeper: A Reality Check on U.S. Government Forecasts for a Lasting Tight Oil & Shale Gas Boom*. Santa Rosa, CA: Post Carbon Institute, 2014.
4. Papageorgiou LG. Supply chain optimisation for the process industries: advances and opportunities. *Comput Chem Eng*. 2009;33:1931–1938.
5. Garcia DJ, You F. Supply chain design and optimization: challenges and opportunities. *Comput Chem Eng*. 2015;81:153–170.
6. Weijermars R. Value chain analysis of the natural gas industry: lessons from the US regulatory success and opportunities for Europe. *J Nat Gas Sci Eng*. 2010;2:86–104.
7. Seydor SM, Clements E, Pantelemonitis S, Deshpande V. *Understanding the Marcellus Shale Supply Chain*. Pittsburgh, PA: University of Pittsburgh, Katz Graduate School of Business, 2012.
8. Laurenzi IJ, Jersey GR. Life cycle greenhouse gas emissions and freshwater consumption of marcellus shale gas. *Environ Sci Technol*. 2013;47:4896–4903.
9. Calderón AJ, Guerra OJ, Papageorgiou LG, Siirola JJ, Reklaitis GV. Financial considerations in shale gas supply chain development. In: Krist V, Gernaey JKH, Rafiqul G, editors. *Computer Aided Chemical Engineering*. Volume 37. Elsevier, 2015:2333–2338.
10. Gracceva F, Zeniewski P. Exploring the uncertainty around potential shale gas development – a global energy system analysis based on TIAM (TIMES Integrated Assessment Model). *Energy*. 2013;57:443–457.
11. Jayakumar R, Rai R. Impact of Uncertainty in Estimation of Shale-Gas-Reservoir and Completion Properties on EUR Forecast and Optimal Development Planning: A Marcellus Case Study. *Society of Petroleum Engineers*. DOI:10.2118/162821-PA.
12. Chaudhri MM. Numerical Modeling of Multifracture Horizontal Well for Uncertainty Analysis and History Matching: Case Studies From Oklahoma and Texas Shale Gas Wells. *Society of Petroleum Engineers*. DOI:10.2118/153888-MS.
13. Harding NR. Application of Stochastic Prospect Analysis for Shale Gas Reservoirs. *Society of Petroleum Engineers*. DOI:10.2118/114855-MS.
14. Yang L, Grossmann IE, Manno J. Optimization models for shale gas water management. *AIChE J*. 2014;60:3490–3501.
15. Cafaro DC, Grossmann IE. Strategic planning, design, and development of the shale gas supply chain network. *AIChE J*. 2014;60:2122–2142.
16. Gao J, You F. Optimal design and operations of supply chain networks for water management in shale gas production: MILFP model and algorithms for the water-energy nexus. *AIChE J*. 2015;61:1184–1208.
17. Yang L, Grossmann IE, Mauter MS, Dilmore RM. Investment optimization model for freshwater acquisition and wastewater handling in shale gas production. *AIChE J*. 2015;61:1770–1782.
18. Gao J, You F. Shale gas supply chain design and operations toward better economic and life cycle environmental performance: MINLP model and global optimization algorithm. *ACS Sustain Chem Eng*. 2015;3:1282–1291.
19. Heath GA, O'Donoughue P, Arent DJ, Bazilian M. Harmonization of initial estimates of shale gas life cycle greenhouse gas emissions for electric power generation. *Proc Natl Acad Sci*. 2014;111:E3167–E3176.
20. Weber CL, Clavin C. Life cycle carbon footprint of shale gas: review of evidence and implications. *Environ Sci Technol*. 2012;46:5688–5695.
21. Dale AT, Khanna V, Vidic RD, Bilec MM. Process based life-cycle assessment of natural gas from the marcellus shale. *Environ Sci Technol*. 2013;47:5459–5466.
22. Swindell GS. Marcellus Shale in Pennsylvania: A 2,600 Well Study of Estimated Ultimate Recovery. In: *SPE Annual Meeting*. Dallas, TX, 2014.[
23. Sahinidis NV. Optimization under uncertainty: state-of-the-art and opportunities. *Comput Chem Eng*. 2004;28:971–983.
24. Bertsimas D, Brown DB, Caramanis C. Theory and applications of robust optimization. *SIAM Rev*. 2011;53:464–501.
25. Ben-Tal A, Nemirovski A. Robust optimization – methodology and applications. *Math Program*. 2002;92:453–480.

26. You F, Wassick JM, Grossmann IE. Risk management for a global supply chain planning under uncertainty: models and algorithms. *AIChE J*. 2009;55:931–946.
27. Gebreslassie BH, Yao Y, You F. Design under uncertainty of hydrocarbon biorefinery supply chains: multiobjective stochastic programming models, decomposition algorithm, and a comparison between CVaR and downside risk. *AIChE J*. 2012;58:2155–2179.
28. You F, Grossmann IE. Multicut Benders decomposition algorithm for process supply chain planning under uncertainty. *Ann Oper Res*. 2013;210:191–211.
29. Shapiro A, Homem-de-Mello T. A simulation-based approach to two-stage stochastic programming with recourse. *Math Program*. 1998;81:301–325.
30. Kleywegt AJ, Shapiro A, Homem-de-Mello T. The sample average approximation method for stochastic discrete optimization. *SIAM J Optim*. 2002;12:479–502.
31. Shapiro A. Monte Carlo sampling methods. In: Ruszczynski A, Shapiro A, editors. *Handbooks in Operations Research and Management Science*. Volume 10. Oxford, UK: Elsevier, 2003:353–425.
32. Slutz JA, Anderson JA, Broderick R, Horner PH. Key Shale Gas Water Management Strategies: An Economic Assessment. In: International Conference on Health Safety and Environment in Oil and Gas Exploration and Production, Perth, Australia, 2012.
33. He C, You F. Toward more cost-effective and greener chemicals production from shale gas by integrating with bioethanol dehydration: novel process design and simulation-based optimization. *AIChE J*. 2015;61:1209–1232.
34. He C, You F. Shale gas processing integrated with ethylene production: novel process designs, exergy analysis, and techno-economic analysis. *Ind Eng Chem Res*. 2014;53:11442–11459.
35. EIA US. Natural Gas Consumption by End Use. 2015, Accessed 5/20, 2015. Available at: http://www.eia.gov/dnav/ng/ng_cons_sum_dcu_nus_m.htm.
36. EIA. Underground Natural Gas Storage. Accessed 9/29, 2014. Available at: http://www.eia.gov/pub/oil_gas/natural_gas/analysis_publications/ngpipeline/undrgrnd_storage.html.
37. EIA. *Levelized Cost and Levelized Avoided Cost of New Generation Resources in the Annual Energy Outlook 2015*. Washington, DC: U.S. Energy Information Administration, 2015.
38. National Academy of Engineering NRC, Committee on America's Energy Future, Division on Engineering and Physical Sciences. *America's Energy Future: Technology and Transformation*. Washington, DC: National Academies Press, 2009.
39. Birge JR. State-of-the-art-survey—stochastic programming: computation and applications. *INFORMS J Comput*. 1997;9:111–133.
40. You F, Castro PM, Grossmann IE. Dinkelbach's algorithm as an efficient method to solve a class of MINLP models for large-scale cyclic scheduling problems. *Comput Chem Eng*. 2009;33:1879–1889.
41. Chu Y, You F. Integration of production scheduling and dynamic optimization for multi-product CSTRs: generalized Benders decomposition coupled with global mixed-integer fractional programming. *Comput Chem Eng*. 2013;58:315–333.
42. Wei J, Realff MJ. Sample average approximation methods for stochastic MINLPs. *Comput Chem Eng*. 2004;28:333–346.
43. Oracle. Oracle Crystal Ball. Accessed 6/19, 2015. Available at: http://www.oracle.com/appserver/business-intelligence/crystalball/index.html.
44. Yue D, Kim MA, You F. Design of sustainable product systems and supply chains with life cycle optimization based on functional unit: general modeling framework, mixed-integer nonlinear programming algorithms and case study on hydrocarbon biofuels. *ACS Sustain Chem Eng*. 2013;1:1003–1014.
45. Liu S, Simaria AS, Farid SS, Papageorgiou LG. Optimising chromatography strategies of antibody purification processes by mixed integer fractional programming techniques. *Comput Chem Eng*. 2014;68:151–164.
46. Yue D, Guillen-Gosalbez G, You F. Global optimization of large-scale mixed-integer linear fractional programming problems: a reformulation-linearization method and process scheduling applications. *AIChE J*. 2013;59:4255–4272.
47. Zhong Z, You F. Globally convergent exact and inexact parametric algorithms for solving large-scale mixed-integer fractional programs and applications in process systems engineering. *Comput Chem Eng*. 2014;61:90–101.
48. Gong J, You F. Global optimization for sustainable design and synthesis of algae processing network for CO2 mitigation and biofuel production using life cycle optimization. *AIChE J*. 2014;60:3195–3210.
49. Garcia DJ, You F. Network-based life cycle optimization of the net atmospheric CO2-eq ratio (NACR) of fuels and chemicals production from biomass. *ACS Sustain Chem Eng*. 2015;3:1732–1744.
50. Birge JR, Louveaux FV. A multicut algorithm for two-stage stochastic linear programs. *Eur J Oper Res*. 1988;34:384–392.
51. Slyke RMV, Wets R. L-shaped linear programs with applications to optimal control and stochastic programming. *SIAM J Appl Math*. 1969;17:638–663.
52. Birge JR, Louveaux F. *Introduction to Stochastic Programming*. New York, NY: Springer, 2011.
53. Kali P, Wallace SW. *Stochastic Programming*. Chichester: Wiley Press, 1994.
54. Ladlee J, Jacquet J. The implications of multi-well pads in the Marcellus Shale. *Community and Regional Development Institute at Cornell (CaRDI) Research and Policy Brief Series*. 2011;43. Available at: http://www2.cce.cornell.edu/naturalgasdev/documents/pdfs/policy_brief_sept11-draft02.pdf.
55. Marcellus-Shale.us. Real Marcellus Gas Production. 2013; Accessed 8/29, 2014. Available at: http://www.marcellus-shale.us/Marcellus-production.htm.
56. Biegler LT, Grossmann IE, Westerberg AW. *Systematic Methods of Chemical Process Design*. Upper Saddle River, NJ: Prentice Hall PTR, 1997.
57. Brooke A, Kendrick DA, Meeraus A, Rosenthal RE. *GAMS: A User's Guide*. Washington, DC: Course Technology, 1988.
58. Yue D, You F. Game-theoretic modeling and optimization of multi-echelon supply chain design and operation under Stackelberg game and market equilibrium. *Comput Chem Eng*. 2014;71:347–361.
59. EIA. Natural Gas Consumption by End Use. Accessed 6/16, 2015. Available at: http://www.eia.gov/dnav/ng/ng_cons_sum_dcu_spa_a.htm.
60. EIA. Heat Content of Natural Gas Consumed. Accessed 6/16, 2015. Available at: http://www.eia.gov/dnav/ng/ng_cons_heat_dcu_nus_a.htm.
61. EIA. High value of liquids drives U.S. producers to target wet natural gas resources. 2014; Accessed 5/20, 2015, http://www.eia.gov/todayinenergy/detail.cfm?id=16191#.
62. Jiang M, Hendrickson CT, VanBriesen JM. Life cycle water consumption and wastewater generation impacts of a marcellus shale gas well. *Environ Sci Technol*. 2014;48:1911–1920.
63. DOE. Energy Efficiency & Renewable Energy. Accessed 6/16, 2015. Available at: http://www.regulations.doe.gov/certification-data/CCMS-81578122497.html.
64. EIA. Gas furnace efficiency has large implications for residential natural gas use. Accessed 6/16, 2015.Available at: http://www.eia.gov/todayinenergy/detail.cfm?id=14051.
65. Steven L, Thekdi A. *Industrial Natural Gas Energy Efficiency Calculator Tools*. Sempra Energy – Southern California Gas Company. CEC-500-2014-066, San Diego, CA, 2013.

Appendix A

In this section, we provide the input data of the Case Studies Section (Table A1).

Table A1. Input Data for the Case Studies

Parameter	Indices	Value	Reference
dl_t(Mscf/year)	–	2000–3000	Ref. 59
$dm_{m,t}$(Mscf/year)	$m1$	87,934–107,474	Ref. 59
	$m2$	50,011–61,125	
	$m3$	34,258–41,871	
	$m4$	55,699–68,076	
ect(MJ/Mscf)	–	1,105	Ref. 60
$eur_{i,js}$	–	2.46–49.79	Refs. 1 and 22
lc_i	–	0.05–0.15	Ref. 15
$lpm_{p,m}$(mile)	–	5–30	Ref. 15
$lsp_{i,p}$(mile)	–	5–30	Ref. 15
mc_i	–	0.85–0.95	Ref. 15
pef	–	0.97	Ref. 15
pl_t(\$/Mscf gas)	–	20–40	Ref. 61
prc_r(Mscf/year)	$r1$	12,000,000	Ref. 34
	$r2$	120,000,000	
	$r3$	1,200,000,000	
pri_r(\$)	$r1$	40,326,500	Ref. 34
	$r2$	160,542,690	
	$r3$	639,131,600	

TABLE A1. *Continued*

Parameter	Indices	Value	Reference
sdc_i(\$/well)	–	270,000–292,000	Ref. 62
$spc_{i,t}$(\$/Mscf)	–	1.2–1.4	Ref. 62
$spp_{i,\tau}$(Mscf/year)	–	$spp_{i,\tau}=a\cdot t^b$; a:16,000–18,000; b: −0.37	Ref. 15
tln	–	12	Refs. 54,59
tmn_i	–	48	Ref. 54
$tprc_r$(Mscf/year)	$r1$	64,094	Ref. 15
	$r2$	402,213	
	$r3$	2,600,166	
	$r4$	16,809,161	
$tpri_r$(Mscf/year)	$r1$	45,954	Ref. 15
	$r2$	138,327	
	$r3$	423,871	
	$r4$	1,297,056	
ue_m	$m1$	0.50	Refs. 63–65
	$m2$	0.64	
	$m3$	0.80	
	$m4$	0.76	
vp(\$/Mscf)	–	3.6	Ref. 34
vtcm(\$/Mscf)	–	0.003	Refs. 15 and 62
vtcs(\$/Mscf)	–	0.003	Refs. 15 and 62

Appendix B

In this work, we propose a novel solution algorithm integrating parametric approach and L-shaped method to tackle the two-stage SMILFP problem. In the inner loop of this novel algorithm, a classical L-shaped method is implemented. By solving the dual-problem of the original subproblem in the inner iteration, we are able to obtain the corresponding Benders cut and update solution to the master problem. In this section, we present the detailed model formulation of both the dual-subproblem and Benders cuts

$$\begin{aligned}\max\ fsub=&\sum_{i\in I}\sum_{t\in T} NN_{i,t}^{\text{fix}}\cdot \text{eur}_{i,js}\cdot \text{spp}_{i,t}\cdot umb1_{i,t}\\ &-\sum_{i\in I}\sum_{p\in P}\sum_{t\in T}\sum_{r\in R}\text{TPC}_{i,p,r}^{\text{fix}}\cdot \text{vcp1}_{i,p,t}\\ &-\sum_{p\in P}\sum_{m\in M}\sum_{t\in T}\sum_{r\in R}\text{TPMC}_{p,m,r}^{\text{fix}}\cdot \text{vcp2}_{p,m,t}\\ &-\sum_{p\in P}\sum_{t\in T}\sum_{r\in R}\text{PC}_{p,r}^{\text{fix}}\cdot \text{vcp3}_{p,t}\\ &+\sum_{m\in M}\sum_{t\in T} dm_{m,t}\cdot \text{vcp4}_{m,t}\\ &+\sum_{t\in T} dl_t\cdot \text{vcp5}_t\end{aligned} \tag{B1}$$

$$\text{s.t.}\rightarrow umb1_{i,t}+umb2_{i,t}\le\frac{\text{spc}_{i,t}}{(1+dr)^t} \tag{B2}$$

$$-umb4_{p,t}+\text{vcp5}_t\le-\frac{\text{pl}_t}{(1+dr)^t} \tag{B3}$$

$$-umb3_{p,t}+umb5_{p,t}\le 0 \tag{B4}$$

$$\begin{aligned}&-umb2_{i,t}+\text{pef}\cdot\text{mc}_i\cdot umb3_{p,t}+\text{pef}\cdot\text{lc}_i\\ &\cdot umb4_{p,t}-\text{vcp1}_{i,p,t}-\text{vcp3}_{p,t}\\ &\le\frac{\text{vp}+\text{vtcs}\cdot\text{lsp}_{i,p}}{(1+dr)^t}\end{aligned} \tag{B5}$$

$$umb6\le -uc \tag{B6}$$

Where $umb1_{i,t}$, $umb2_{i,t}$, $umb3_{p,t}$, $umb4_{p,t}$, $umb5_{p,t}$, $umb6$ are dual variables corresponding to original mass-balance constraints (11), (12), (13), (14), (15), and (10), respectively. Similarly, $\text{vcp1}_{i,p,t}$, $\text{vcp2}_{p,m,t}$, $\text{vcp3}_{p,t}$, $\text{vcp4}_{m,t}$, vcp5_t are dual variables corresponding to original capacity constraints (16), (17), (18), (19), and (20), respectively. After solving the subproblem, the corresponding optimality cut and feasibility cut can be calculated by the following equations:

Optimality Cut

$$\begin{aligned}\theta\ge&\sum_{m\in M}\sum_{t\in T}\text{dm}_{m,t}\cdot\text{vcp4}_{m,t}^{\text{fix}}+\sum_{m\in M}\sum_{t\in T}\text{dl}_t\cdot\text{vcp5}_t^{\text{fix}}\\ &+\text{eur}_{i,js}\cdot\text{spp}_{i,t}\cdot umb1_{i,t}^{\text{fix}}\cdot NN_i\\ &-\text{vcp1}_{i,p,t}^{\text{fix}}\cdot\text{TPC}_{i,p,r}-\text{vcp2}_{p,m,t}^{\text{fix}}\cdot\text{TPMC}_{p,m,r}-\text{vcp3}_{p,t}^{\text{fix}}\cdot PC_{p,r}\end{aligned} \tag{B7}$$

Feasibility Cut

$$\begin{aligned}&\sum_{m\in M}\sum_{t\in T}\text{dm}_{m,t}\cdot\text{vcp4}_{m,t}^{\text{fix}}+\sum_{m\in M}\sum_{t\in T}\text{dl}_t\cdot E5_t^{\text{fix}}\\ &+\text{eur}_{i,js}\cdot\text{spp}_{i,t}\cdot umb1_{i,t}^{\text{fix}}\cdot NN_i\\ &-vcp1_{i,p,t}^{\text{fix}}\cdot\text{TPC}_{i,p,r}-\text{vcp2}_{p,m,t}^{\text{fix}}\cdot\text{TPMC}_{p,m,r}-\text{vcp3}_{p,t}^{\text{fix}}\cdot\text{PC}_{p,r}\le 0\end{aligned} \tag{B8}$$

By adding these newly generated cuts to the master problem, we can solve the updated master problem to obtain an updated solution, which further leads to the updates of lower and upper bounds for this two-stage SMILFP problem.

Appendix C

In this section, we present the detailed design decisions obtained by solving the deterministic model, which is given by the following Figure 1C.

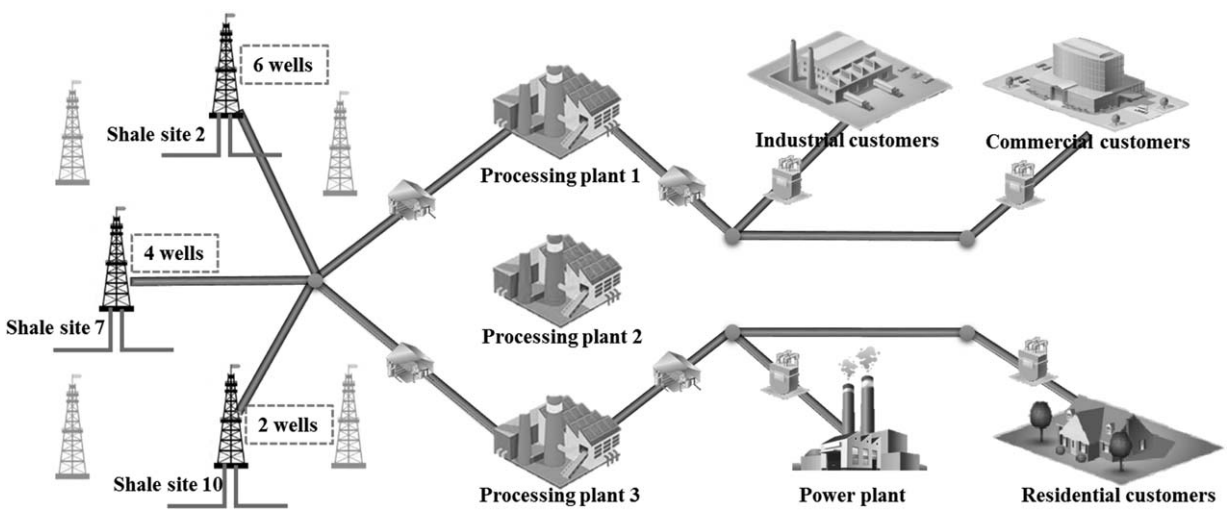

Figure C1. Optimal design of shale gas supply chain network for deterministic model.

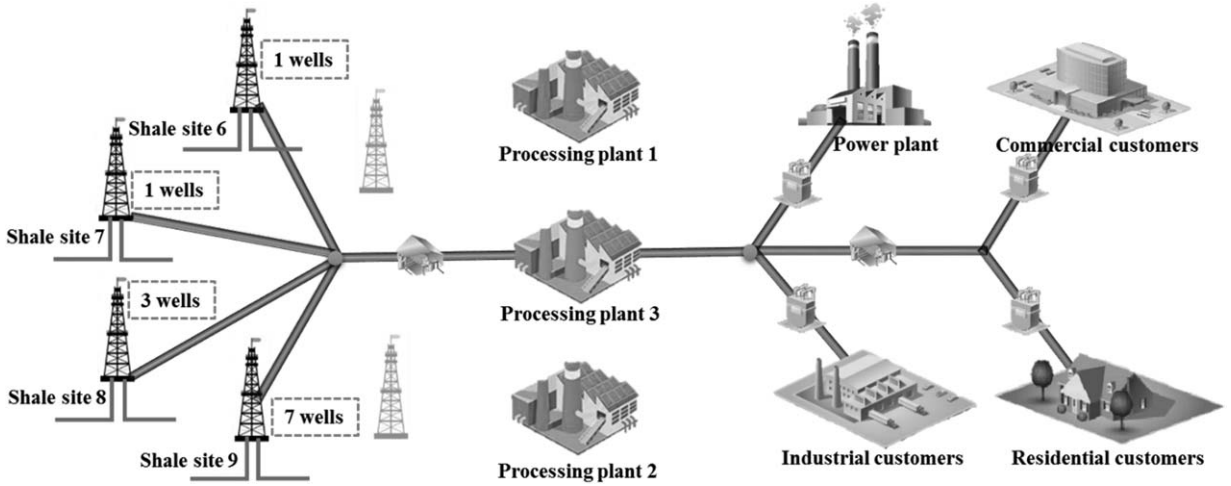

Figure D1. Optimal design of shale gas supply chain network under EUR uncertainty for SMILP model.

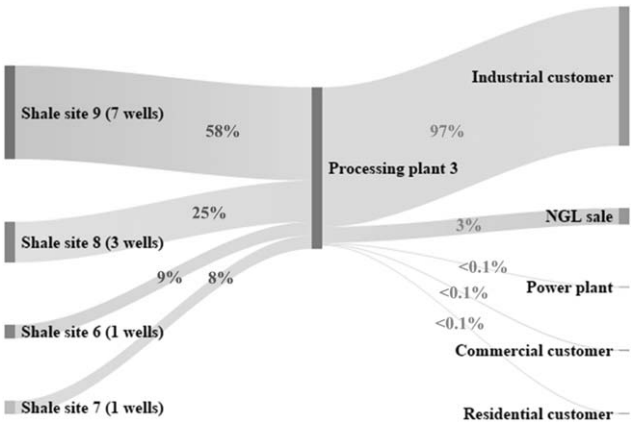

Figure D2. Sankey diagram of shale gas flow in the supply chain network for SMILP model.

As can be seen in Figure 1C, although the same shale sites are chosen, the number of wells being drilled in each shale site is different. The main difference regarding the design decisions is on the construction of the processing plants. In the two-stage SMILFP model, only processing plant 2 is constructed, while in the deterministic model, both processing plant 1 and processing plant 3 are constructed with 5.0 Bscf/year and 5.2 Bscf/year processing capacity, respectively. As a result, the downstream distribution of natural gas is different. Natural gas from processing plant 1 will be transported to industrial and commercial customers for end-use. Meanwhile, processing plant 3 targets on satisfying the demand of power plants and residential customers. The different design decisions of deterministic model result in the sacrifice of economic efficiency when the EUR uncertainty is taken into account, causing a 31% higher unit cost of energy in the deterministic model than the stochastic programming one.

Appendix D

In this section, we summarize the difference between solutions from the proposed SMILFP model and that from a SMILP model. The objectives of them are minimizing the LCOE generated from shale gas and minimizing the total cost, respectively. A similar optimal shale gas supply chain network can be obtained from this SMILP model, as shown in Figure 1D.

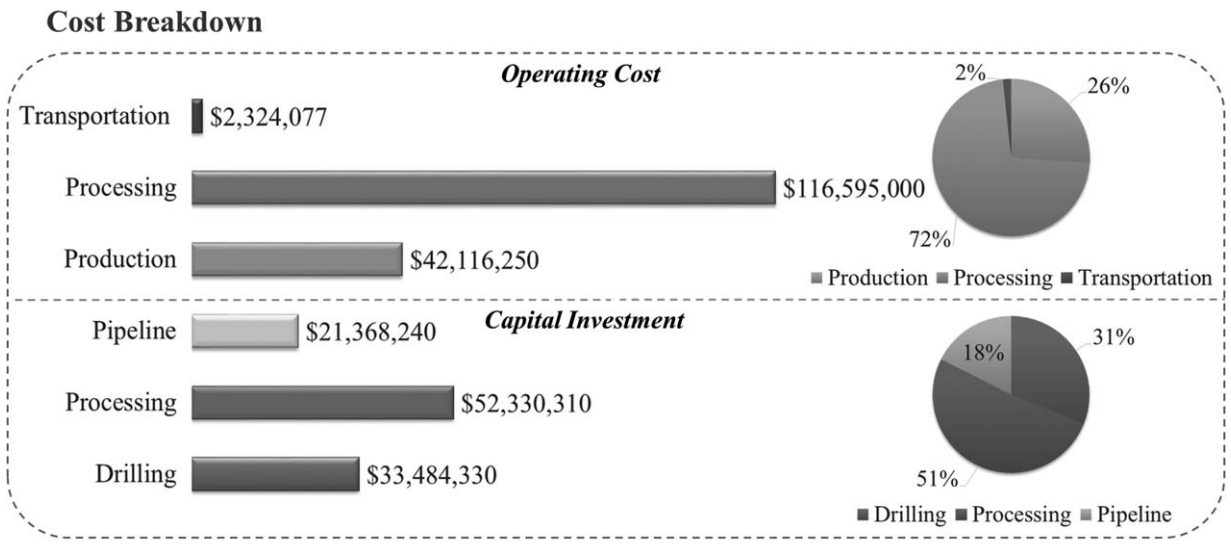

Figure D3. Cost breakdown regarding capital investment and operating cost for SMILP model.

As can be seen, the major difference is about the drilling schedule. Shale sites 6, 7, 8, and 9 are chosen for shale gas production, and up to seven wells are drilled in shale site 9. In the SMILP model, the processing plant 3 is constructed with identical capacity to processing plant 2 as in the SMILFP model. Although the total cost of the SMILP model is 2.2% lower due to a 9.6% reduction in shale gas production, the corresponding LCOE is \$0.0041/MJ, 11% higher than \$0.0037/MJ obtained from SMILFP model.

The expected shale gas flow is presented in a similar Sankey diagram as shown in Figure D2. As can be seen, as in the SMILP model, the only objective is minimizing the total cost without considering economic efficiency. Thus, almost all of the natural gas is transported to the nearest customer, known as industrial customer in this specific case study, to save corresponding transportation cost and investment. Obviously, a more balanced end-use distribution of natural gas can be obtained by solving the SMILFP model against the SMILP one.

At last, we present the cost breakdown of the solution to this SMILP model in Figure D3. As can be observed, although the exact costs for different process in this shale gas supply chain are different, the overall cost breakdowns for both operating cost as well as capital investment remain the same.

To conclude, first of all the SMILP model verifies some of the results obtained from the proposed SMILFP model, namely the supply chain design and cost breakdown. Meanwhile, the advantage of SMILFP model over the SMILP model in obtaining more meaningful solutions is demonstrated through the analysis of shale gas flow and LCOE.

Manuscript received June 29, 2015, and revision received Aug. 23, 2015.